Molecular Motion of Polyethylene Chain Ends Tethered to a Fresh Surface of Poly(tetrafluoroethylene) *in Vacuo*

Masato Sakaguchi*

Ichimura Gakuen College, 61, Uchikubo, Inuyama 484, Japan

Shigetaka Shimada and Katsuhiro Yamamoto

Nagoya Institute of Technology, Gokiso, Nagoya 466, Japan

Masahiro Sakai

Instrument Center, Institute for Molecular Science, Myodaiji, Okazaki 444, Japan

Received April 8, 1996; Revised Manuscript Received August 13, 1996[⊗]

ABSTRACT: The molecular motion of polyethylene (PE) chain ends tethered to a fresh surface of poly(tetrafluoroethylene) (PTFE) *in vacuo* was studied. The tethered PE chain ends were produced by a block copolymerization of PTFE with ethylene *in vacuo* at 77 K. Each of the tethered PE chains has an unpaired electron at the growing chain end. The mobility of the tethered PE chain ends was observed in the range of 2.8−95 K by an electron spin resonance (ESR) spectrometer with the unpaired electron as a probe. The inter exchange motion between two α protons at the chain ends probably occurs at 2.8 K. The site exchange motion between two conformations at the chain ends occurs above 7 K and is more clearly observed at 15 K. Moreover, the torsional oscillation of the β proton occurs above 30 K. Furthermore, the rotation of the chain end about the chain axis of PE probably occurs at 95 K. The assignment of molecular motion modes was based on spectral simulations. The high mobility of the tethered PE chain ends is attributed to (1) a large space around the chains; (2) the presence of the vacuum; (3) the lack of chain aggregation, because the concentration of the chain ends is low and they are tethered; and (4) the immiscibility of PE and PTFE. The ends of PE chains tethered on the PTFE *in vacuo* probably behave as isolated PE chain ends *in vacuo*, and may reveal the mobility intrinsic to PE chain ends.

Introduction

Many studies on the molecular motion of polymer chains in bulk or in solution have been reported. In these systems, the mobility of the polymer chains depends greatly on their surroundings. For example, the mobility of chains in bulk relates to the amount and size of the free volume. The free volume may be influenced by interactions with inter- and intrapolymer chains. In solution, the mobility is affected by an interaction between the polymer chains and solvent molecules. Thus the polymer chains do not reveal the mobility intrinsic to an individual chain but rather reflect the features of the surroundings. Increased attention is here focused on a fundamental understanding of the physical properties of isolated molecules.

In low molecular weight compounds, numerous studies on the molecular motion of isolated molecules have been reported[1] in which the small molecules are trapped in an argon matrix that is produced by a simultaneous condensation of argon with gaseous molecules. The mobility of the molecules is high even at 4 K because the molecules are isolated by a frozen argon matrix that has very weak interaction with the molecules. The mobility is high, but some of the motion may be suppressed in the frozen argon matrix.

In polymer materials, it is impossible to get a gaseous polymer. Thus isolated polymer chains in a frozen argon matrix cannot be obtained.

The polymer chains which are included in the channels of inclusion complexes such as urea[2] and perhydrotriphenylene[3−7] are isolated from neighboring polymer chains by the host matrix. However, conformation of the chains is restricted by the channel wall. Thus, the mobility of the included chains reflects a specific conformation such as the *trans* form for polyethylene (PE),[4−7] and some of the motions may be restrained in the channel.

If polymer chains have the following features, they are scarcely affected by other chains and can be regarded as "isolated polymer chains" *in vacuo:* (1) a large space around the chains, (2) the presence a vacuum, and (3) an inhibition of the chain aggregation.

In our previous two papers (1) the PE alkyl radical, $CH_2CH_2^{\bullet}$, tethered to the poly(tetrafluoroethylene) (PTFE) surface has high mobility, even at a temperature as low as 77 K,[8] and (2) the peroxy radicals at the terminal of a PE chain tethered to a PTFE surface also have high mobility.[9] The high mobility of the two kinds of PE chain ends was interpreted as an extremely low segmental concentration of PE molecules on the PTFE surface.

PE chains tethered to a fresh surface of PTFE *in vacuo* can be regarded as "isolated PE chains" *in vacuo* for the following reasons: (1) the concentration of PE chains is extremely low on the PTFE surface; (2) the PE chains are present *in vacuo*; (3) the aggregation of PE chains is prevented by linkage to the PTFE surface with a covalent bond; and (4) PE and PTFE are immsicible. These details are described in later sections. Each of the tethered PE chains has an unpaired electron at the chain terminal. The mobility of the tethered PE chain ends with the unpaired electron as a probe can be observed by an ESR spectrometer.

We have reported[10] a preliminary result for the molecular motion of PE chain ends tethered to a PTFE surface *in vacuo.* In the present study, a detailed analysis of the molecular motion of tethered PE chain ends is discussed.

[⊗] Abstract published in *Advance ACS Abstracts,* May 15, 1997.

S0024-9297(96)00514-1 CCC: $14.00

Experimental Section

PTFE powder (Aflon G80, Asahi Glass Co., Ltd.) was used without further purification. Ethylene monomer (Takachiho Co., Ltd.) was purified by a freeze−pump−thaw method.

The PE chains tethered to a fresh surface of PTFE *in vacuo* were produced as follows: The PTFE powder (1.53 g) was fractured with ethylene (5.2×10^{-4} mol) at 77 K *in vacuo* by a homemade vibration glass-ball mill.[11] The ball milling of PTFE powder produces PTFE mechano radicals,[11] which are chain-end type radicals located on the fresh surface[12] produced by the fracture. The PTFE mechano radicals can initiate a radical polymerization of ethylene at 77 K *in vacuo*.[13] Ethylene monomer is supplied to the PE-propagating radicals by physical mixing under the milling; the radical polymerization of ethylene continues, and then the PE chains tethered to the PTFE fresh surface *in vacuo* are produced. Thus, polymerized PE chains at 77 K have unpaired electrons at the chain terminals. After the polymerization, the powder sample was dropped into an ESR sample tube at 77 K, which was connected to the glass-ball mill.

An ESR spectrometer (BRUKER ESP 300E) equipped with a helium cryostat (OXFORD ESR 900) was used to investigate the molecular motion of the tethered PE chains. ESR spectra were observed at X-band frequency, at a microwave power level of 2 μW to avoid power saturation, and with 100 kHz field modulation. The magnetic field was calibrated by NMR Gauss meter (BRUKER ER035M with F1 probe head). Temperatures were controlled by a temperature controller (OXFORD ITC 4).

The sample in the ESR sample tube was cooled to 2.8 K in the cryostat and left to stand for 120 min; then the ESR spectrum was observed at 2.8 K. The sample was kept at each of the elevated temperatures for 15 min for observation.

Spectral Simulation

Hori et al. have reported[14] a computer program based on a conformation exchange due to a ring inversion of the cyclohexyl radicals, a secondary radical with one α proton (H_α). This program employs the line shape equation derived by Heinzer[15] based on a density matrix theory in the Liouville representation. Heinzer's equation is, as expected, identical with that derived from the modified Bloch equations.

We have modified the computer program developed by Hori et al. to simulate ESR spectra of a primary alkyl radical, $CH_2CH_2^\bullet$, which has two H_αs and two β protons (H_β).

The molecular coordinate system (x, y, z) based on the principal axis (A_x, A_y, A_z) of the hyperfine splitting (hfs) tensor is defined by the nuclear spin of one H_α. On a common coordinate, A_x is parallel to p_π occupied by the unpaired electron at the α carbon (C_α), A_z is along the direction of the $C_\alpha-H_\alpha$ bond, and A_y lies in the $H_{\alpha1}-C_\alpha-H_{\alpha2}$ plane and is perpendicular to both A_x and A_z (Figure 1).

When the hfs term arises from two H_αs, the A_x, A_y, and A_z need to be respectively replaced by A_1, A_2, A_3 defined by a new molecular coordinate system (1, 2, 3) which reflects a spatial relationship between two H_αs. A_2 lies in the $C_\alpha-C_\beta-C_\gamma$ plane and bisects the $H_{\beta2}-C_\beta-H_{\beta1}$ bond angle. A_1 is both perpendicular to the $C_\alpha-C_\beta-C_\gamma$ plane and A_2. A_3 is perpendicular to both A_1 and A_2 and is parallel to the chain axis of PE. There are two conformations for the tethered PE chain ends, called site 1 and site 2. At site 1, each A_x of $H_{\alpha1}$ or $H_{\alpha2}$ is parallel to p_π and tilts from axis 1 with an angle of $\phi = 15°$. A_z lies in the $H_{\alpha1}-C_\alpha-H_{\alpha2}$ plane and tilts from axis 3 with $\theta = -90°$ for $H_{\alpha1}$ and $\theta = 30°$ for $H_{\alpha2}$. At site 2, A_y and A_z are the same as at site 1, except each A_x of $H_{\alpha1}$ or $H_{\alpha2}$ tilts $\theta = -15°$ from axis 1.

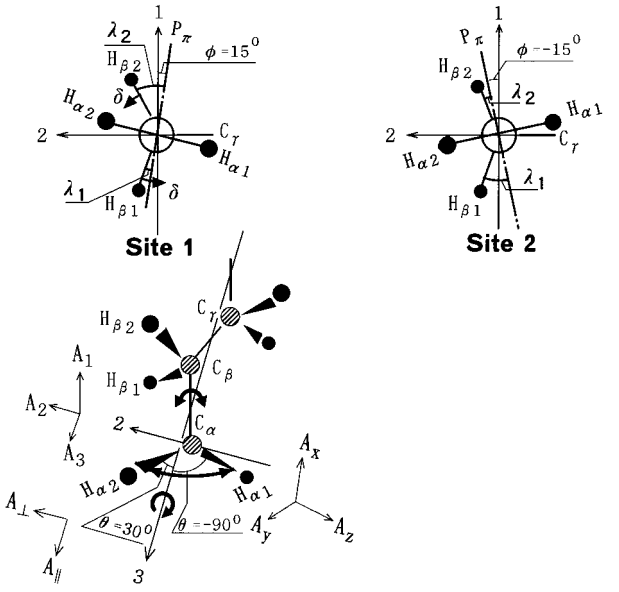

Figure 1. Two sites of the tethered PE chain ends. Three types of molecular coordinate based on the principal axes of the hfs tensor of H_α (A_1, A_2, A_3), ($A_{||}$, $A_\perp$), and (A_x, A_y, A_z) are shown. Details are given in the text.

When another coordinate is based on a rotation mode around the axis 3, $A_{||}$ is parallel to A_3. $A_\perp$ is derived from the average of A_1 and A_2, and is perpendicular to $A_{||}$.

Figure 2a shows the ESR powder pattern of the model alkyl radical, $RCH_2^\bullet$, simulated by $A_x = 2.0$ mT, $A_y = 3.20$ mT, $A_z = 1.00$ mT[16], and $\theta = 30°$ for $H_{\alpha2}$ and $\theta = -90°$ for $H_{\alpha1}$. The simulated spectrum was obtained from the conformations of site 1 and site 2 except for the two H_βs (Figure 1), in which an equal population at each site and a frozen molecular motion were assumed. Figure 2b spectrum was calculated as in Figure 2a except for the interexchange beteen two H_αs in the $H_{\alpha1}-C_\alpha-H_{\alpha2}$ plane at a rapid rate (10 GHz). From Figure 2b spectrum, $A_1 = 1.90$ mT, $A_2 = 1.48$ mT, and $A_3 = 2.77$ mT are obtained. These A_1, A_2, and A_3 mean "preaveraged" hfs constants are from A_x, A_y, and A_z under the rapid interexchange motion. Figure 2c spectrum was simulated by the preaveraged hfs constants. The peak positions are identical with those in the Figure 2b spectrum. The spectral shape is fairly identical. Thus A_x, A_y, and A_z can be replaced by the preaveraged hfs constants, when H_α is in the rapid interexchange motion mode. The hfs constants of H_α are listed in Table 1.

The following major simulations are carried out using preaveraged hfs constants and a site exchange rate described in a later section, because our simulation program is limited to a single exchange rate.

Results and Discussion

The observed spectrum at 2.8 K is shown in Figure 3 with curve A. Curve B is simulated from the conformation of site 1 and site 2 (Figure 1). Site 1 is defined as $\phi = 15°$, $\lambda_1 = 15°$, and $\lambda_2 = 45°$, where λ_1 or λ_2 is a projection angle between p_π and $H_{\beta1}$ or $H_{\beta2}$ to the 1−2 plane. Site 2 is defined as $\phi = -15°$, $\lambda_1 = 45°$, and $\lambda_2 = 15°$. The spectrum based on site 1 was obtained by hfs constants of H_α; $A_x = 2.00$ mT, $A_y = 3.20$ mT, $A_z = 1.00$ mT with relation to $\theta = -90°$ for $H_{\alpha1}$ and $\theta = 30°$ for $H_{\alpha2}$ and hfs constants of H_β; and $A_{\beta1} = 3.86$ mT and $A_{\beta2} = 2.07$ mT, which were derived by the McConnell equation[20] with $\lambda_1 = 15°$ for $H_{\beta1}$ and $\lambda_2 = 45°$ for $H_{\beta2}$.

Table 1. Proton Hyperfine Splitting Constants of Model Radicals $RCH_2^{\bullet}$

hyperfine splitting (mT) of H_α			hyperfine splitting (mT) of H_β		
			$A_{\beta1}(\lambda_1)$	$A_{\beta2}(\lambda_2)$	
A_x	A_y	A_z			
2.00	3.20	1.00	3.86	2.07	frozen state
A_1	A_2	A_3			
1.90	1.48	2.77	3.86	2.07	rapid interexchange of H_α
$A_\perp$	$A_\perp$	$A_\parallel$			
1.69	1.69	2.77	3.86	2.07	rotation around A_3 axis

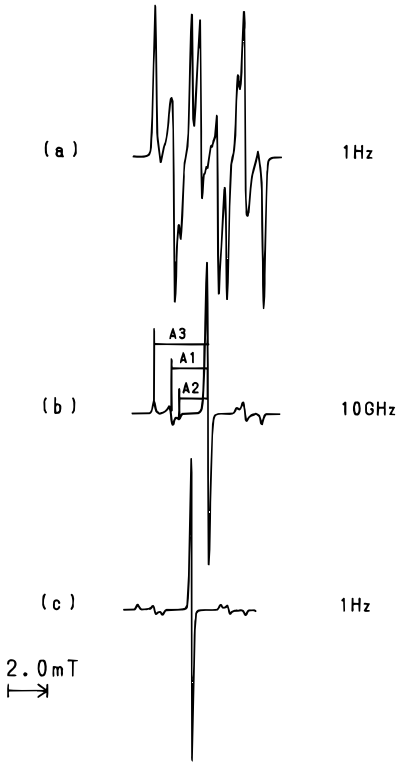

Figure 2. Simulated ESR spectra from model radical $RCH_2^{\bullet}$. (a) Powder spectrum based on $A_x = 2.00$ mT, $A_y = 3.20$ mT, and $A_z = 1.00$ mT, and $\theta = -90°$ for $H_{\alpha1}$ and $\theta = 30°$ for $H_{\alpha2}$. The simulated spectrum was obtained from the conformations of site 1 ($\phi = 15°$) and site 2 ($\phi = -15°$), except for two H_βs, in which an equal population at each site and a frozen molecular motion are assumed. (b) Simulated as in part a except H_α causes interexchange motion in the $H_{\alpha1}-C_\alpha-H_{\alpha2}$ plane at a rate of 10 GHz. The preaveraged hfs constants $A_1 = 1.90$ mT, $A_2 = 1.48$ mT, and $A_3 = 2.77$ mT, were obtained from the drawn spectrum of part b. (c) Simulated by the preaveraged hfs constants $A_1 = 1.90$ mT, $A_2 = 1.48$ mT, and $A_3 = 2.77$ mT. This simulated spectrum is shifted to a lower magnetic field to avoid superposition of the center peak.

Another spectrum based on site 2 was obtained as in site 1 except $A_{\beta1} = 2.07$ mT ($\lambda_1 = 45°$) for $H_{\beta1}$ and $A_{\beta2} = 3.86$ mT ($\lambda_2 = 15°$) for $H_{\beta2}$. Each simulated spectrum derived from site 1 or 2 was obtained by assuming an equal population and a frozen molecular motion. The simulated spectrum derived from site 1 was, as expected, identical with the spectrum derived from site 2. Curve B, based on the frozen molecular motion, is a poor fit to the observed spectrum. This result suggests that some kind of molecular motion occurs.

Curve C is simulated as in curve B, except for the interexchange motion between two H_αs in the $H_{\alpha1}-C_\alpha-H_{\alpha2}$ plane at a rapid rate (10 GHz). This simulated spectrum is in good agreement with the observed spectrum, suggesting that the inter exchange motion occurs even at 2.8 K. Curve D is simulated as in curve B, except for the preaveraged hfs constants of $A_1 = 1.9$ mT, $A_2 = 1.48$ mT, and $A_3 = 2.77$ mT, derived from the model radical assuming the rapid interexchange motion. This simulated spectrum is also in good agreement with the observed spectrum. Thus the good agreement of curve C with curve D means that the A_x, A_y, and A_z can be replaced by the preaveraged values, A_1, A_2, and A_3, respectively, when the rapid interexchange motion occurs.

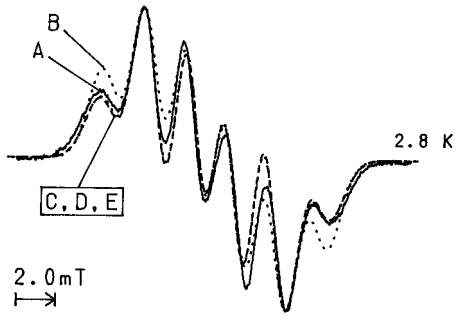

Figure 3. Observed and simulated spectra of PE chain ends tethered to a PTFE surface. Curve A (—): observed at 2.8 K. Curve B (· · ·): simulated by assuming frozen molecular motion. Curve C (· · ·): simulated as in curve B except for the rapid interexchange motion of H_α. Curve D (- - -): simulated as in curve B except for the preaveraged hfs constants $A_1 = 1.90$ mT, $A_2 = 1.48$ mT, and $A_3 = 2.77$ mT, which are derived from assuming the rapid interexchange motion. Curve E (- - -): simulated as in curve B except for $A_\parallel = 2.77$ mT and $A_\perp = 1.69$ mT, which are derived from assuming the rotation around the PE chain axis.

Curve E is simulated as in curve B, except $A_\parallel = 2.77$ mT and $A_\perp = 1.69$ mT, derived from the model radical rotating about axis 3, which is the chain axis of PE. This simulated spectrum is also in good agreement with the observed spectrum. This agreement suggests that the PE chain ends rotate around the chain axis. If a fine structure in the line shape of the ESR spectrum was observed, a more detailed analysis for a molecular motion mode could be carried out by a spectral simulation. Unfortunately, the line shape of the spectrum was unaltered with even low modulation width.

Adrian et al. have reported[1a] that H_α of *n*-propyl radical, $CH_3CH_2CH_2^{\bullet}$, in argon matrix is an interexchange motion mode at 4 K. Moreover, Kasai has reported[1d] that H_α of trimethylene oxide anion, O^--$CH_2CH_2^{\bullet}$, in argon matrix is also the interchange motion mode at 4 K.

Thus, we may conclude that the interexchange motion mode is more reasonable than the rotational motion mode at 2.8 K.

The spectral simulations at 2.8 K are based on the isotropic hfs term ($A_{\alpha iso} = 2.07$ mT) of H_α and $\rho_c B_2 = 4.14$ mT, where B_2 is the empirical parameter used in the McConnel equation[20] and ρ_c is the spin density at C_α. These values are too small compared to the typical values, $A_{\alpha iso} = 2.25-2.30$ mT and $\rho_c B_2 = 5.0-5.38$ mT[1a,b,d,19] for primary alkyl radicals. Initially, we conducted various trials using typical values to simulate the ESR spectrum at 2.8 K, but we failed to obtain any appropriate simulation spectrum. Generally, these

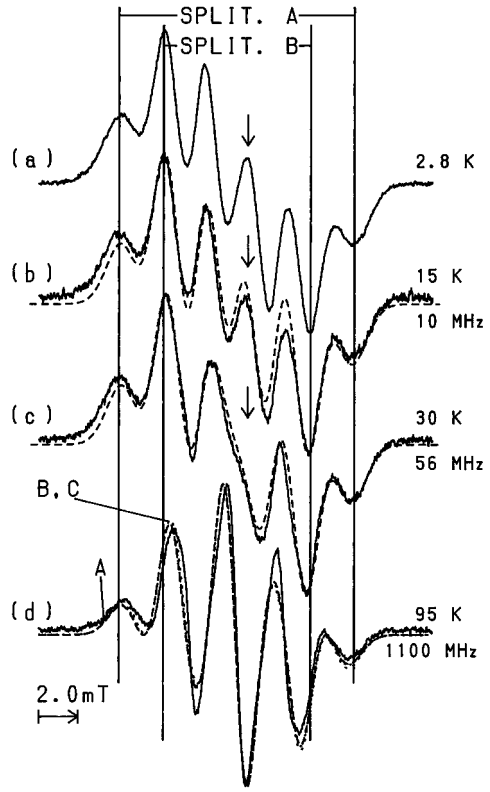

Figure 4. Observed and simulated spectra of tethered PE chain ends. spectrum obesrved at (a) 2.8 K and (b) (—) at 15 K. Spectra (· · ·) simulated as in curve D in Figure 3 except the site exchange rate is 10 MHz. (c) Spectra (—) observed at 30 K. Spectra (- - -) simulated as in the broken line in part b except the site exchange rate is 56 MHz and the oscillation amplitude of H_β is 7°. (d) Curve A (—) is the spectra observed at 95 K. Curve B (- - -) is the spectra simulated as in the broken line in part c except the site exchange rate is 1100 MHz and the oscillation amplitude is 13°. Curve C (· · ·) is the spectra simulated as in curve B, except $A_{\parallel} = 2.77$ mT and $A_{\perp} = 1.69$ mT. SPLIT.A and SPLIT.B are indicators of spectral width.

values are dependent on ρ_c, which is affected by the substituent on the radical and the matrix surrounding the radical. These too small values may be attributed to a low ρ_c.

The ESR spectra observed at 2.8, 15, and 30 K are shown in Figure 4a,b,c with solid lines. The intensity of the peak shown with the arrow decreases with an increase in temperature, and the spectrum changes from six lines to five lines. Spectral changes beginning at 7 K (not shown) are clearly evident at 15 K and continue with increasing temperatures to 95 K. This spectral change was reversible in the temperature range 2.8−95 K. The intensity of the spectrum was obtained by a double integration of the ESR spectrum. The ESR intensities with the temperature-increasing process are identical with those in the decreasing process (Figure 5). This result indicates that the concentration does not change in each temperature range. Thus the spectral change is attributed to a temperature dependence on the molecular motion of the tethered PE chains. The simulated spectrum (the broken line in Figure 4b) was obtained as in curve D in Figure 3, except the site exchange rate between site 1 and site 2 is 10 MHz. The 15 K simulated spectrum is in good agreement with the observed spectrum. Thus the site exchange motion occurs at 15 K (Table 2). Some site exchange rates determined by spectral simulations are plotted against the inverse observation temperatures (Figure 6). The

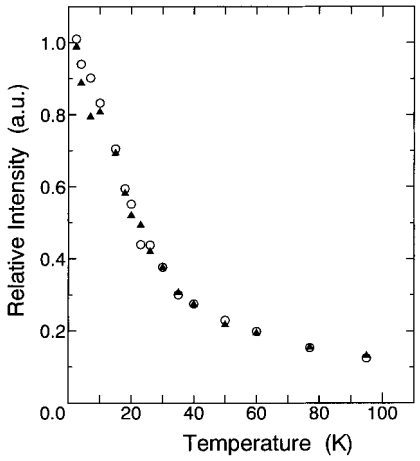

Figure 5. Relative intensities of ESR spectra from the tethered PE chains are plotted against observation temperatures on the increasing process (○) and the decreasing process (▲).

activation energy (E_p) of the site exchange motion is estimated as 260 J/mol.

SPLIT.A and SPLIT.B shown in Figure 4 are indicators of the width of the ESR spectrum. Figure 7 shows changes of SPLIT.A and SPLIT.B values caused by temperature. The decreases of both values begin around 30 K and continue with increasing temperature to 95 K. The decrease is obvious in the observed spectrum at 95 K (Figure 4d).

Hori et al. have reported[14] a temperature dependence of A_β as follows. The magnitude of A_β is calculated from the well-known McConnel equation[20]

$$A_\beta = B_o + \rho_c B_2 \cos^2(\lambda + \delta) \quad (1)$$

where λ is the dihedral angle of the $C_\beta-H_\beta$ bond axis relative to p_π and δ is an amplitude of the torsional oscillation of H_β around the equilibrium state. B_0 and B_2 are empirical parameters. B_0 is neglected in the following discussion. Under the condition of an identical $\langle\delta^2\rangle$ all each H_β, the following equation is given

$$A_{\beta i} = 1/2 b_2\{1 + \cos 2\lambda_i(1 - 2\langle\delta^2\rangle)\} \quad (2)$$

where $i = 1$ or 2 and $b_2 = \rho_c B_2$. Considering the oscillation, $A_{\beta av}$ is given as

$$A_{\beta av} = 1/2(A_{\beta 1} + A_{\beta 2}) = b_2\{1 + 1/2 \cos(2\lambda_1 - \pi/3) - \langle\delta^2\rangle \cos(2\lambda_1 - \pi/3)\} \quad (3)$$

where a dihedral angle of 120° between two H_βs is assumed. Equation 3 indicates that $A_{\beta av}$ approaches b_2 from $b_2\{1 + 1/2 \cos(2\lambda_1 - \pi/3)\}$ with an increase in temperature under the oscillation. In other words, the decrease of $A_{\beta av}$ will exhibit decreases of SPLIT.A and SPLIT.B with increasing temperature when torsional oscillation occurs.

The ESR spectrum observed at 30 K is shown with the solid line in Figure 4c. The broken line in Figure 4c is simulated as the broken line in Figure 4b, except the site exchange rate equals 56 MHz and $A_{\beta 1} = 3.81$ mT and $A_{\beta 2} = 2.07$ mT based on the torsional motion mode (Table 2). The good agreement between the observed and simulated spectra indicates that torsional oscillation occurs at 30 K. An oscillation amplitude of

Table 2. Proton Hyperfine Splitting Constants and Oscillation Amplitudes Determined by Simulation

temp (K)	site hyperfine splitting (mT)			exchange rate (MHz)	hyperfine splitting (mT)			oscillation amp (deg)
	A_1	A_2	A_3		$A_{\beta 1}(\lambda_1)$	$A_{\beta 2}(\lambda_2)$	A_{β}av	
2.8	1.90	1.48	2.77		3.86	2.07	2.96	0
15	1.90	1.48	2.77	10	3.86	2.07	2.96	0
30	1.90	1.48	2.77	56	3.81	2.07	2.94	7
95	1.90	1.48	2.77	1100	3.33	2.43	2.88	13

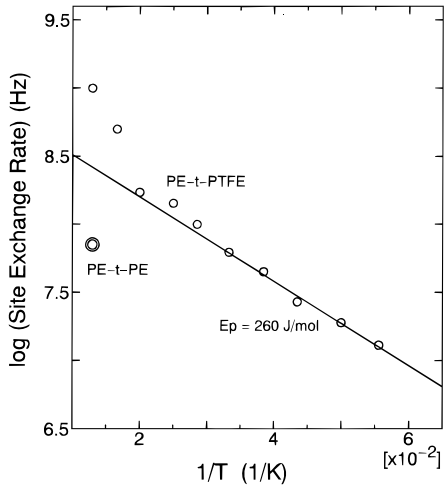

Figure 6. Temperature dependence of the site exchange rate calculated by simulation. PE-t-PTFE: PE chains tethered to a PTFE surface. PE-t-PE: PE chains tethered to a PE surface.

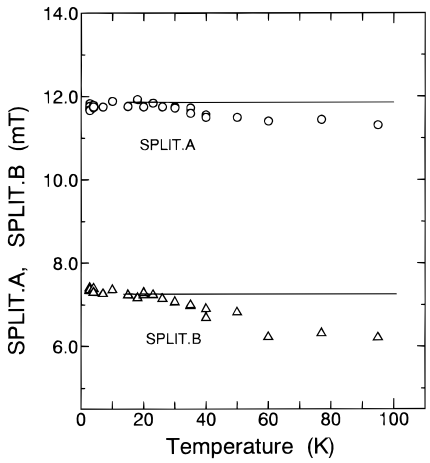

Figure 7. Temperature dependence of SPLIT.A (○) and SPLIT.B (△) values.

7° was estimated by eq 3 with $b_2 = 4.14$ mT and $A_{\beta \mathrm{av}} = 2.94$ mT, which were determined by spectral simulation. Figure 8 shows a temperature dependence of $A_{\beta 1}$, $A_{\beta 2}$, and $A_{\beta \mathrm{av}}$. The decrease of $A_{\beta \mathrm{av}}$ with increasing temperature indicates that the oscillation of H_β occurs above 30 K. The decreases of SPLIT.A and SPLIT.B with increasing temperature (Figure 7) provide additional evidence for the oscillatory motion mode.

The observed spectrum at 95 K is shown with curve A in Figure 4d. Curve B is simulated as in the broken line in Figure 4c, except the site exchange rate equals 1100 MHz, $A_{\beta 1} = 3.33$ mT, and $A_{\beta 2} = 2.43$ mT. The oscillation amplitude is 13°. This simulated spectrum is in good agreement with the observed spectrum. Curve C in Figure 4d is calculated as in curve B, except for the axially symmetric hfs constants, $A_{||} = 2.77$ mT and $A_{\perp} = 1.69$ mT, derived from an assumption of the rotation around the PE chain axis. Curve C is also in good agreement with the observed spectrum, indicating that the PE chain ends rotate around the chain axis.

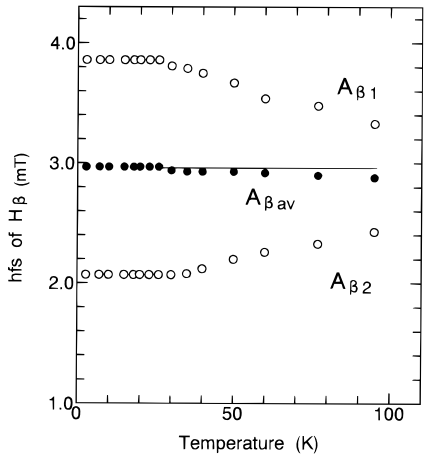

Figure 8. Temperature dependence of $A_{\beta 1}$, $A_{\beta 2}$, and $A_{\beta \mathrm{av}}$ calculated by the simulation.

In this case, if a fine structure in the line shape of the ESR spectrum is observed, more detailed analysis for a molecular motion mode could be carried out by spectral simulation. Unfortunately, the line shape of the spectrum did not change with even low modulation width. It was difficult in this case to assign a motion mode. However, considering the large oscillation amplitude of H_β around the equilibrium, the tethered PE chain ends probably rotate around the chain.

The polymerization degree of the tethered PE chains could not be estimated. However, the area per tethered point on the PTFE surface (3.1×10^3 A^2/point) was estimated from the radical concentration (6.8×10^{16} spins/g) and the specific surface area (2.1 m^2/g).[10] This large surface area per tethered point suggests that the tethered PE chains have a large free space around the chains, i.e., the concentration of tethered PE chains to PTFE is extremely low.

We have reported[8] that the molecular motion of the PE chains tethered to a "PE surface" is suppressed even at 77 K and shows a slow site exchange rate of 71 MHz. This site exchange rate is much slower compared to 1000 MHz for the PE chain ends tethered to a PTFE surface (Figure 6). The slow site exchange rate of PE chain ends tethered to the PE surface indicates that the molecular motion of the PE chain ends is strongly affected by the PE surface because PE is miscible with PE. The slow site exchange rate also suggests that the molecular motion of the chain ends relates not only to the local motion at the chain end but also to the entire motion of the tethered chains. Thus the high molecular motion of the PE chain ends tethered to a PTFE surface *in vacuo* may exhibit the mobility intrinsic to PE chain ends.

Concluding Remarks

The molecular motion of PE chain ends tethered to a PTFE surface *in vacuo* was observed by an ESR spectrometer. The assignment of following molecular motion modes was based on spectral simulations: (1) an interexchange motion of H_α at 2.8 K, (2) a site

exchange motion between two conformations at the PE chain end above 7 K, (3) an oscillation of H_β above 30 K, and (4) a rotation around the PE chain axis at 95 K. The high mobility of the ends of tethered PE chains is attributed to (1) a large space around the chains; (2) the presence of the vacuum; (3) prevention of chain aggregation, because concentration of the chain ends is low and they are tethered; and (4) the immiscibility of PE and PTFE. The ends of PE chains tethered on the PTFE *in vacuo* probably behave as isolated PE chain ends *in vacuo* and may reveal the mobility intrinsic to PE chain ends.

Acknowledgment. We would like to thank Dr. Hori for his valuable discussion.

References and Notes

(1) For example: (a) Adrian, F. J.; Cochran, E. L.; Bowers, V. A. *J. Chem. Phys.* **1973**, *59*, 3946. (b) Kasai, P. H. *J. Am. Chem. Soc.* **1972**, *94*, 5950. (c) Davidson, R. B.; Miyagawa, I. *J. Chem. Phys.* **1970**, *52*, 1727. (d) Kasai, P. H. *J. Am. Chem. Soc.* **1990**, *112*, 4313.

(2) Hori, Y.; Shimada, S.; Kashiwabara, H. *Polymer* **1977**, *18*, 1143.

(3) Sozzani, P.; Behling, R. W.; Schilling, F. C.; Brucker, S.; Helfand, E.; Bovey, F. A.; Jelinski, L. W. *Macromolecules* **1989**, *22*, 3318.

(4) Sozzani, P.; Bovey, F. A.; Schilling, F. C. *Macromolecules* **1991**, *24*, 6764.

(5) Schilling, F. C.; Amundson, K. R.; Sozzani, P. *Macromolecules* **1994**, *27*, 6498.

(6) Tonelli, A. E. *Macromolecules* **1990**, *23*, 3134.

(7) Zhan, Y.; Mattice, W. L. *Macromolecules* **1992**, *25*, 4078.

(8) Sakaguchi, M.; Yamaguchi, T.; Shimada, S.; Hori, Y *Macromolecules* **1993**, *26*, 2612.

(9) Shimada, S.; Suzuki, A.; Sakaguchi, M.; Hori, Y. *Macromolecules* **1996**, *29*, 973.

(10) Sakaguchi, M.; Shimada, S.; Hori, Y.; Suzuki, A.; Kawaizumi, F.; Sakai, M.; Bandow, S. *Macromolecules* **1995**, *28*, 8450.

(11) Sakaguchi, M.; Sohma, J. *J. Polym. Sci. Polym. Phys. Ed.* **1975**, *13*, 1233.

(12) Kurokawa, N.; Sakaguchi, M.; Sohma, J. *Polym. J.* **1978**, *10*, 93.

(13) Sakaguchi, M.; Sohma, J. *J. Appl. Polym. Sci.* **1978**, *22*, 2915.

(14) Hori, Y.; Shimada, S.; Kashiwabara, H. *J. Phys. Chem.* **1986**, *90*, 3037.

(15) Heinzer, J. *Mol. Phys.* **1971**, *22*, 167.

(16) The hfs constants used in the simulation were obtained as follows: The hfs constants of H_α of an alkyl radical are well-understood and typically assumed:[1d,17,18,19] $A_x = 2.20$ mT, $A_y = 3.50$ mT, $A_z = 1.20$ mT, and the isotropic hfs term, $A_{\alpha\mathrm{iso}} = 2.30$ mT.[1d] Their characteristic reduced values ($A'_x = 0.96$, $A'_y = 1.52$, and $A'_z = 0.52$) are obtained by a normalization to $A_{\alpha\mathrm{iso}} = 2.30$ mT. We used the hfs constants in the simulation, $A_x = 2.0$ mT, $A_y = 3.20$ mT, and $A_z = 1.00$ mT, which are estimated from similar reduced value, $A'_x = 0.97$, $A'_y = 1.55$, and $A'_z = 0.48$, by a normalization to $A_{\alpha\mathrm{iso}} = 2.07$ mT.

(17) McConnell, H. M.; Strathedee, J. *Mol. Phys.* **1959**, *2*, 129.

(18) Kasai, P. H. *J. Am. Chem. Soc.* **1972**, *94*, 5950.

(19) Fessenden, R. W.; Schuler, R. *J. Phys. Chem.* **1963**, *39*, 2147.

(20) Heller, C.; McConnell, H. M. *J. Chem. Phys.* **1960**, *32*, 1535.

MA960514B